



## 2D crystal structure, magnetic behavior and theoretic analysis of two new molecular solids based on Ni(maleonitriledithiolate)<sub>2</sub> monoanion with substituted 2-aminopyridinium

Yong Hou<sup>a</sup>, Wen-Tao Yin<sup>a</sup>, Xiao-Dan Xie<sup>a</sup>, Xing Chen<sup>a</sup>, Jia-Rong Zhou<sup>a</sup>, Hong-Rong Zuo<sup>a</sup>, Qian Huang<sup>a</sup>, Le-Min Yang<sup>a</sup>, Chun-Lin Ni<sup>a,\*</sup>, Xue-Lei Hu<sup>b</sup>

<sup>a</sup> Department of Applied Chemistry, Centre of Inorganic Functional Materials, College of Science, South China Agricultural University, 510642 Guangzhou, PR China

<sup>b</sup> School of Chemical Engineering and Pharmacy, Wuhan Institute of Technology, 430073 Wuhan, PR China

### ARTICLE INFO

#### Article history:

Received 25 August 2009

Received in revised form 5 November 2009

Accepted 9 November 2009

Available online 14 November 2009

#### Keywords:

Bis(maleonitriledithiolate)nickelate(III) anion

Substituted 2-aminopyridinium

Crystal structure

Magnetic properties

Spin-gap transition

### ABSTRACT

Two new molecular solids, [BzPyNH<sub>2</sub>][Ni(mnt)<sub>2</sub>](**1**) and [2-NpCH<sub>2</sub>PyNH<sub>2</sub>][Ni(mnt)<sub>2</sub>](**2**) (mnt<sup>2-</sup> = maleonitriledithiolate, [BzPyNH<sub>2</sub>]<sup>+</sup> = 1-benzyl-2-aminopyridinium and [2-NpCH<sub>2</sub>PyNH<sub>2</sub>]<sup>+</sup> = 1-(2'-naphthylmethylene)-2-aminopyridinium) have been characterized structurally and magnetically. The Ni(III) ions of **1** and **2** form a 1D magnetic chain within a [Ni(mnt)<sub>2</sub>]<sup>-</sup> column through Ni···N or π···π interactions. Some weak interactions observed in **1** and **2** give further rise to a 2D structure. The overlapping fashions of the [Ni(mnt)<sub>2</sub>]<sup>-</sup> anions are different when the 2-aminopyridine ring was fixed and the phenyl ring changed into the naphthyl ring of the cation. Magnetic susceptibility measurements in the temperature range 2–300 K show that **1** is weak antiferromagnetic coupling, while **2** exhibits a novel and interesting spin-gap transition around 140 K with Δ/k<sub>B</sub> = 381.4 K.

© 2009 Elsevier B.V. All rights reserved.

### 1. Introduction

The magnetic, super-conducting and optical properties of molecular solids based on [M(dithiolate)<sub>2</sub>] (M = Ni, Pd, or Pt ions) have been the focus of considerable current attention [1–5]. Coomber and co-workers in 1996 discovered that NH<sub>4</sub>Ni(mnt)<sub>2</sub>·H<sub>2</sub>O shows a ferromagnetic behavior below 4.5 K, suggesting that magnetic exchange between [Ni(mnt)<sub>2</sub>]<sup>-</sup> anions is very sensitive to not only the overlap fashion of neighboring [Ni(mnt)<sub>2</sub>]<sup>-</sup> anions but also intermolecular contacts, and small structural change can result in large changes in the materials properties of molecular solids based on the [Ni(mnt)<sub>2</sub>]<sup>-</sup> monoanion [6]. Substituted benzylpyridinium derivatives have been proved to be multifunctional counter-cation of [M(mnt)<sub>2</sub>]<sup>-</sup> anion, which may make the anions a diverse number of stacking and overlapping modes and results in versatile magnetic properties such as ferromagnetic ordering at low-temperature, magnetic transition, meta-magnetism, spin-Peierls-like transitions and spin-gap transition [7–12]. These findings have prompted us to further investigate the influence of the substituent groups in the pyridine and benzene rings of the counter-cation on the stacking pattern and magnetic properties of

molecular solids based on [Ni(mnt)<sub>2</sub>]<sup>-</sup> anion. The present work reports crystal structures and magnetic behaviors of two newly prepared molecular solids, [BzPyNH<sub>2</sub>][Ni(mnt)<sub>2</sub>](**1**) and [2-NpCH<sub>2</sub>PyNH<sub>2</sub>][Ni(mnt)<sub>2</sub>](**2**) ([BzPyNH<sub>2</sub>]<sup>+</sup> = 1-benzyl-2-aminopyridinium and [2-NpCH<sub>2</sub>PyNH<sub>2</sub>]<sup>+</sup> = 1-(2'-naphthylmethylene)-2-aminopyridinium). The Ni(III) ions of both **1** and **2** form a 1D zigzag magnetic chain through Ni···N or π···π interactions, while the significantly different overlapping modes of the neighboring [Ni(mnt)<sub>2</sub>]<sup>-</sup> anions resulted in the different magnetic properties that **1** shows antiferromagnetic behavior and **2** exhibits an interesting spin-gap transition around 140 K.

### 2. Experimental

#### 2.1. General materials and techniques

Disodium maleonitriledithiolate (Na<sub>2</sub>mnt), 1-benzyl-2-aminopyridinium bromide ([BzPyNH<sub>2</sub>]<sup>+</sup>Br), and 1-(2'-naphthylmethylene)-2-aminopyridinium bromide ([2-NpCH<sub>2</sub>PyNH<sub>2</sub>]<sup>+</sup>Br) were synthesized following the literature procedures [13,14]. A similar method for preparing [IBzNH<sub>2</sub>Py]<sub>2</sub>[Ni(mnt)<sub>2</sub>] was utilized to prepare [BzPyNH<sub>2</sub>]<sub>2</sub>[Ni(mnt)<sub>2</sub>] and [2-NpCH<sub>2</sub>PyNH<sub>2</sub>]<sub>2</sub>[Ni(mnt)<sub>2</sub>] [15]. C, H and N analyses were performed by a Model 240 Perkin-Elmer instrument. IR spectra were recorded on a Nicolet Avatar 360 FT-IR

\* Corresponding author. Tel.: +86 20 85282568; fax: +86 20 85282366.  
E-mail address: niclchem@scau.edu.cn (C.-L. Ni).

(400–4000  $\text{cm}^{-1}$  region) spectrophotometer in KBr pellets. Variable-temperature magnetic data for **1** and **2** were obtained over the temperature range of 2–300 K using a Quantum Design MPMS-XL super-conducting quantum interference device (SQUID) magnetometer, and the experimental data were corrected for diamagnetism of the constituent atoms estimated from Pascal's constants.

## 2.2. Synthesis of $[\text{BzPyNH}_2][\text{Ni}(\text{mnt})_2](\mathbf{1})$

A  $\text{CH}_3\text{COCH}_3$  solution (10 mL) of  $\text{I}_2$  (140 mg, 0.55 mmol) was slowly added to a  $\text{CH}_3\text{COCH}_3$  solution (50 mL) of  $[\text{BzPyNH}_2]_2[\text{Ni}(\text{mnt})_2]$  (709 mg, 1.0 mmol) and the mixture was stirred for 24 h. The mixture was concentrated under reduced pressure until the volume was reduced to about 20 mL. After initial filtration, to the dark filtration was added 30 mL *i*-PrOH and stored in a refrigerator overnight. About 425 mg of black micro-crystals formed were filtered off, washed with MeOH and dried in vacuum. Yield: 81%. Anal. Calc. for  $\text{C}_{20}\text{H}_{13}\text{NiN}_6\text{S}_4$ : C, 45.81; H, 2.50; N, 16.03. Found: C, 45.77; H, 2.53; N, 15.98%. IR (KBr,  $\text{cm}^{-1}$ ):  $\nu(\text{NH}_2)$ , 3430s;  $\nu(\text{CH}_2)$ , 2924m and 2852m;  $\nu(\text{CN})$ , 2207s;  $\nu(\text{C}=\text{C})$  of  $\text{mnt}^{2-}$ , 1458m.

## 2.3. Synthesis of $[2\text{-NpCH}_2\text{PyNH}_2][\text{Ni}(\text{mnt})_2](\mathbf{2})$

The procedure for preparing **2** was analogous to that for **1**. Yield: 74%. Anal. Calc. for  $\text{C}_{24}\text{H}_{15}\text{NiN}_6\text{S}_4$ : C, 50.19; H, 2.63; N, 14.63. Found: C, 50.23; H, 2.68; N, 14.59%. IR (KBr,  $\text{cm}^{-1}$ ):  $\nu(\text{NH}_2)$ , 3438s;  $\nu(\text{CH}_2)$ , 2919m and 2853m;  $\nu(\text{CN})$ , 2207s;  $\nu(\text{C}=\text{C})$  of  $\text{mnt}^{2-}$ , 1461m.

## 2.4. Crystal structure determination

The single crystals suitable for the X-ray structure analysis of **1** and **2** were obtained by evaporating the solution prepared in

**Table 1**  
Crystallographic Data for **1** and **2**.

Complex	<b>1</b>	<b>2</b>
Empirical formula	$\text{C}_{20}\text{H}_{13}\text{NiN}_6\text{S}_4$	$\text{C}_{24}\text{H}_{15}\text{NiN}_6\text{S}_4$
Formula weight	524.33	574.37
Wavelength (Å)	0.71073	0.71073
Space group	$P2_1/m$	$P2_1/n$
Crystal system	monoclinic	monoclinic
<i>Unit cell dimensions</i>		
<i>a</i> (Å)	8.704(1)	8.101(1)
<i>b</i> (Å)	7.026(1)	23.786(2)
<i>c</i> (Å)	18.466(3)	13.488(1)
$\alpha$ (°)	90	90
$\beta$ (°)	98.67(1)	106.46(1)
$\gamma$ (°)	90	90
<i>V</i> (Å <sup>3</sup> ), <i>Z</i>	1116.4(3), 2	2492.5(4), 4
<i>D</i> <sub>calc</sub> (g/cm <sup>3</sup> )	1.560	1.531
Absorption coefficient	1.264	1.140
<i>F</i> (0 0 0)	534	1172
Crystal size (mm <sup>3</sup> )	0.23 × 0.18 × 0.11	0.23 × 0.18 × 0.12
Maximum and minimum transmission	0.873 and 0.760	0.875 and 0.780
$\theta$ range for data collection (°)	2.2–25.0	1.7–25.0
Limiting indices	$-10 \leq h \leq 9$ $-8 \leq k \leq 8$ $-21 \leq l \leq 21$	$-9 \leq h \leq 9$ $-28 \leq k \leq 27$ $-16 \leq l \leq 16$
Reflections collected	8059	17 982
Independent reflections	2143	4394
( <i>R</i> <sub>int</sub> )	0.040	0.060
Goodness-of-fit (GOF) on <i>F</i> <sup>2</sup>	1.015	1.000
<i>R</i> <sub>1</sub>	0.0343, 0.0399	0.0372, 0.0471
<i>wR</i> <sub>2</sub>	0.1233, 0.1312	0.1012, 0.1061
Largest difference in peak and hole (e Å <sup>-3</sup> )	0.34 and -0.30	0.40 and -0.42

MeCN/*i*-PrOH (*v/v* = 2:1) mixture. Table 1 provides a summary of the crystallographic data for **1** and **2**. Data were collected on a Smart APEX CCD area detector using graphite monochromated

**Table 2**  
Selected bond parameters for **1** and **2**.

Complex	<b>1</b>	<b>2</b>
<i>Bond distances</i> (Å)		
Ni(1)–S(1)	2.1432(10)	2.1464(7)
Ni(1)–S(2)	2.1533(10)	2.1402(7)
Ni(1)–S(3)	2.1455(10)	2.1504(7)
Ni(1)–S(4)	2.1647(10)	2.1501(8)
S(1)–C(2)	1.720(4)	1.717(2)
S(2)–C(3)	1.719(4)	1.719(2)
S(3)–C(6)	1.727(4)	1.720(2)
S(4)–C(7)	1.714(3)	1.721(2)
<i>Bond angles</i> (°)		
S(1)–Ni(1)–S(2)	92.51(4)	92.22(3)
S(1)–Ni(1)–S(4)	87.33(3)	88.04(3)
S(2)–Ni(1)–S(3)	87.42(3)	86.92(3)
S(3)–Ni(1)–S(4)	92.75(3)	92.74(3)
<i>Dihedral angles</i> (°)		
<i>C</i> <sub>Ar</sub> –CH <sub>2</sub> –N <sub>Py</sub> and $\Phi_{\text{Ar}}$ ( $\theta_1$ )	90.0	118.0
<i>C</i> <sub>Ar</sub> –CH <sub>2</sub> –N <sub>Py</sub> and $\Phi_{\text{Py}}$ ( $\theta_2$ )	0	82.1
$\Phi_{\text{Ar}}$ and $\Phi_{\text{Py}}$ ( $\theta_3$ )	90.0	66.3

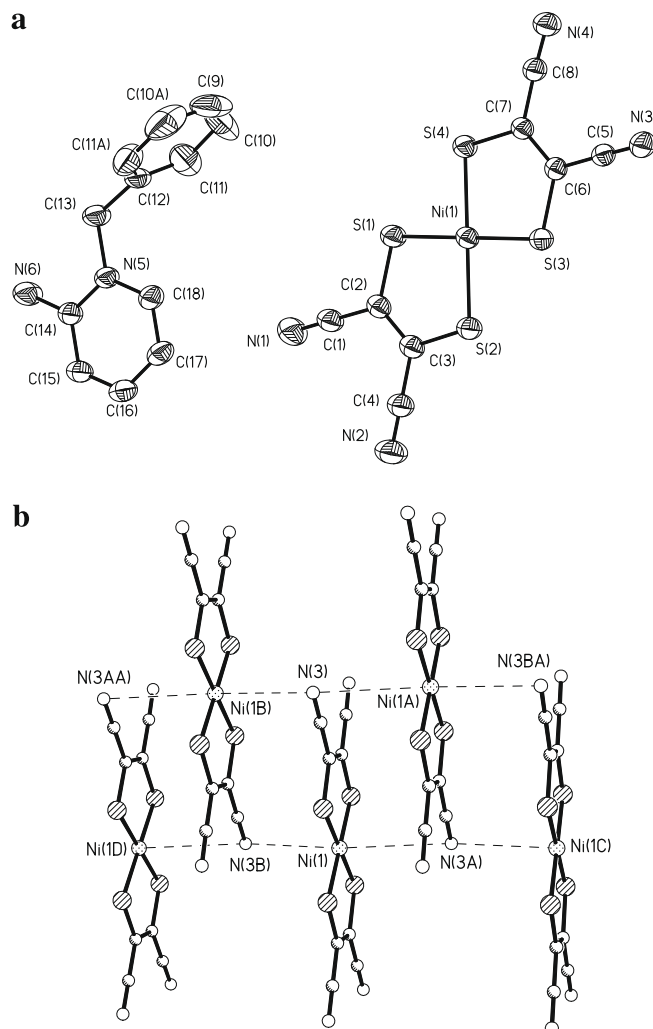


**Fig. 1.** (a) ORTEP plot showing the structure of **1**. (b) Side view of the anions stack of **1** showing the uniform space linear-chain of  $[\text{Ni}(\text{mnt})_2]^{2-}$  anions.

Mo  $K\alpha$  radiation ( $\lambda = 0.71073 \text{ \AA}$ ). The structures were solved by direct methods, and non-hydrogen atoms were refined anisotropically using full matrix least-squares based on  $F^2$ . In two structures, the C–H hydrogen atoms were placed in calculated positions, assigned isotropic thermal parameters,  $U(\text{H}) = 1.2U_{\text{eq}}(\text{C})$ , and allowed to ride on their parent atoms. The N–H hydrogen atoms were located from  $\Delta F$  maps and refined isotropically. All computations were carried out using Bruker's SHELXTL program system [16]. Selected bond lengths and bond angles for **1** and **2** are listed in Table 2.

### 3. Results and discussion

#### 3.1. Crystal structures

An ORTEP drawing of **1** in an asymmetric unit is shown in Fig. 1a with one  $[\text{Ni}(\text{mnt})_2]^-$  anion and a  $[\text{BzPyNH}_2]^+$  cation. The Ni(III) ion in the  $[\text{Ni}(\text{mnt})_2]^-$  anion is coordinated by four sulfur atoms of two  $\text{mnt}^{2-}$  ligands, and exhibits square-planar coordination geometry. The Ni–S bond distance and S–Ni–S bond angles are in agreement with those of the previously reported molecular solids based on  $[\text{Ni}(\text{mnt})_2]^-$  anion [7–12]. In the  $[\text{BzPyNH}_2]^+$  moiety, the dihedral angle of the C(12)–C(13)–N(5) reference plane are  $90.0^\circ(\theta_1)$  for benzene ring and  $0.0^\circ(\theta_2)$  for pyridine ring, respectively. The phenyl ring and the pyridine ring make a dihedral angle of  $90.0^\circ(\theta_3)$ . Within a  $[\text{Ni}(\text{mnt})_2]^-$  anions stacking column, the Ni(III) ions of  $[\text{Ni}(\text{mnt})_2]^-$  anions form a 1D uniform chain with the Ni···Ni distance of  $6.370 \text{ \AA}$  through intermolecular Ni···N, S···C or  $\pi \cdots \pi$  interactions (Fig. 1b). The nearest Ni···N and S···C distances are  $3.604$  and  $3.723 \text{ \AA}$ . The overlapping fashion between neighboring anions along the stacking direction is Ni–N mode (Fig. 2a). Three weak interactions are observed between

**Table 3**  
Intermolecular hydrogen bonds for **1** and **2**.

D–H···A	d(D···H)	d(H···A)	d(D···A)	$\angle(\text{DHA})$
<b>Compound 1</b>				
N(6)–H(6B)···N(4)#1	0.860	2.200	3.054(5)	170.0
N(15)–H(15)···N(3)#1	0.930	2.620	3.332(5)	134.0
<b>Compound 2</b>				
N(6)–H(6A)···N(2)#2	0.860	2.500	2.968(3)	115.0

Symmetry code: #1 =  $x + 1, y, z + 1$ ; #2 =  $-x + 1, -y, -z$ .

$[\text{Ni}(\text{mnt})_2]^-$  anion and  $[\text{BzPyNH}_2]^+$  cation (Table 3): (1) N(6)–H(6B)···N(4)<sup>i</sup> (symmetry code:  $i = x + 1, y, z + 1$ ) hydrogen bond with a N(6)···N(4)<sup>i</sup> distance of  $3.054 \text{ \AA}$ ; (2) C(15)–H(15)···N(3)<sup>ii</sup> (symmetry code:  $ii = x + 1, y, z + 1$ ) hydrogen bond with a C(15)···N(3)<sup>ii</sup> distance of  $3.332 \text{ \AA}$ ; (3)  $\pi \cdots \pi$  interactions between CN group and pyridine ring with a distance of  $3.513 \text{ \AA}$ . These weak interactions give further rise to a 2D structure (Fig. 2b).

In order to investigate effect of the substituted group in the counter-cation on the overlapping fashion of the  $[\text{Ni}(\text{mnt})_2]^-$  anions and the packing pattern of the molecular solids based on  $[\text{Ni}(\text{mnt})_2]^-$  anion,  $[\text{2-NpCH}_2\text{PyNH}_2][\text{Ni}(\text{mnt})_2]$  (**2**) is prepared by utilizing the starting material  $[\text{2-NpCH}_2\text{PyNH}_2]\text{Br}$  instead of  $[\text{BzPyNH}_2]\text{Br}$ . The crystal structural analysis has revealed that the coordination geometries of the anion and cation of **2** are essentially identical to those described above for **1**, while the dihedral angles  $\theta_1, \theta_2$ , and  $\theta_3$  are  $118.0^\circ, 82.1^\circ$  and  $66.3^\circ$  for  $[\text{2-NpCH}_2\text{PyNH}_2]^+$  cation, respectively, which are markedly different from those of **1**. The stacking columns of the anions and the cations for **2** along the direction of  $a$ -axis are shown in Fig. 3a. In a cationic column, the adjacent cations stacked in chair-type conformation (Fig. 3b) and form a 1D column by the  $\pi \cdots \pi$  stacking interactions between the

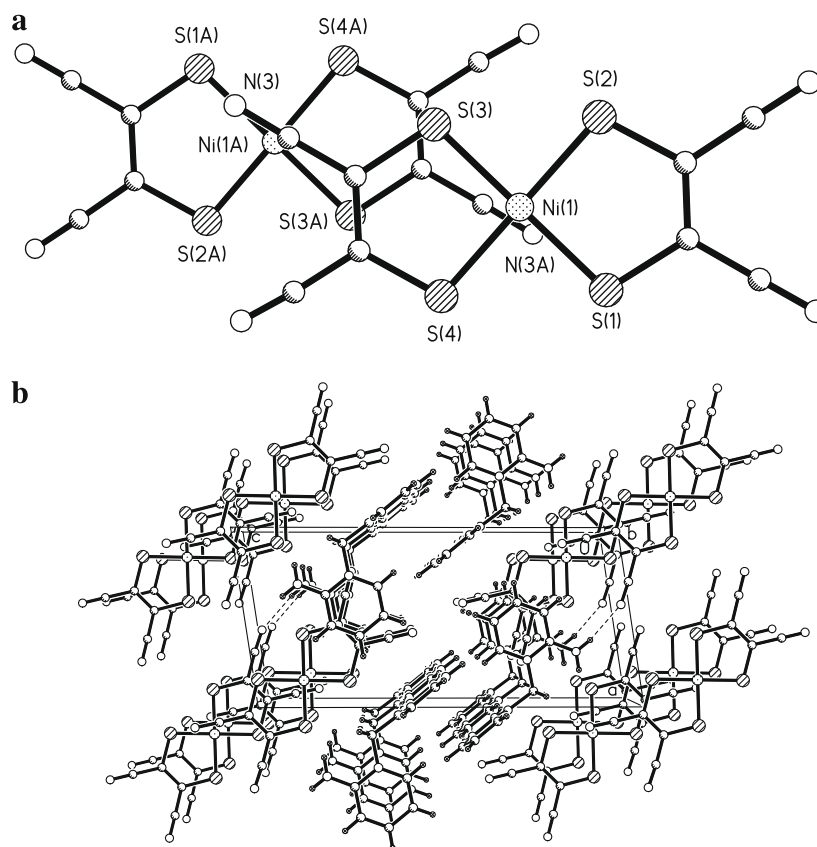


**Fig. 2.** (a) The ring–ring overlapping fashion of  $[\text{Ni}(\text{mnt})_2]^-$  anions of **1**. (b) The packing diagram for **1** as viewed along the  $b$ -axis.

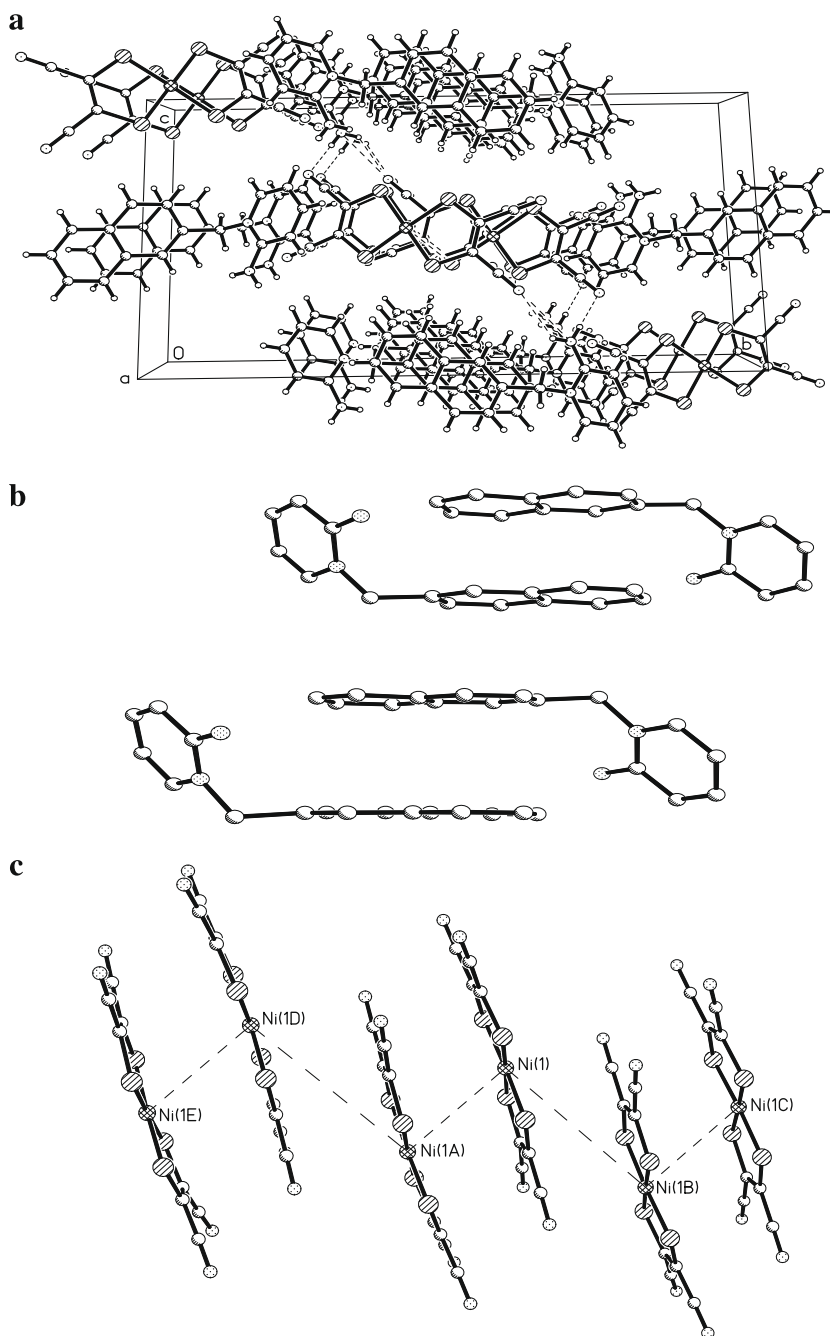


**Fig. 3.** (a) The packing diagram for **2** as viewed along the *a*-axis. (b) Chair-type conformation of the cations in **2**. (c) Side view of the anions stack of **2** showing the alternating space linear-chain of  $[\text{Ni}(\text{mnt})_2]^-$  anions.

naphthyl rings with a vertical distance of 3.626 Å. Within the anion column, the Ni(III) ions form a 1D alternating chain with Ni···Ni distances being 4.201 and 6.617 Å through intermolecular Ni···S, S···S,  $\pi$ ·· $\pi$  interactions (Fig. 3c). Two overlapping fashions of the neighboring  $[\text{Ni}(\text{mnt})_2]^-$  anions are depicted in Fig. 4a and b. The weak N–H···N hydrogen bond between the anion and the cation observed in the **2** (Table 3) results in the formation of 2D structure (Fig. 3a).

From the point of view of structure analysis for **1** and **2**, when we have fixed the 2-aminopyridine ring and changed the phenyl ring into the naphthyl ring, the dihedral angles  $\theta_1$ ,  $\theta_2$ , and  $\theta_3$ , as well as the overlapping modes of the anions in the crystal are markedly different. In addition, some weak interactions in **1** and **2** play important roles in the molecular stacking and magnetic coupling.

### 3.2. Magnetic properties

The variable-temperature (2–300 K) magnetic data for **1** under an applied field of 2000 Oe, expressed as  $\chi_m$  ( $\text{emu mol}^{-1}$ ), are shown in Fig. 5a. As the temperature is lowered, the  $\chi_m T$  value decreased from 0.379 at 300 K to 0.142  $\text{emu K mol}^{-1}$ , indicative of very weak antiferromagnetic exchange. The magnetic susceptibility data in the temperature phase (2–300 K) of **1** can be finely fitted to the Curie-Weiss law with  $C = 0.376 \text{ emu K mol}^{-1}$  and  $\theta = -4.2 \text{ K}$  (the red solid line in Fig. 5a). The very weak antiferromagnetic coupling situation is consistent with the structure of **1**.

For **2**, it is very interesting that the  $\chi_m$  varies in a complex way as the temperature is lowered (Fig. 5b): at first it gradually increase to a maximum at 210 K, and below the temperature the  $\chi_m$  value

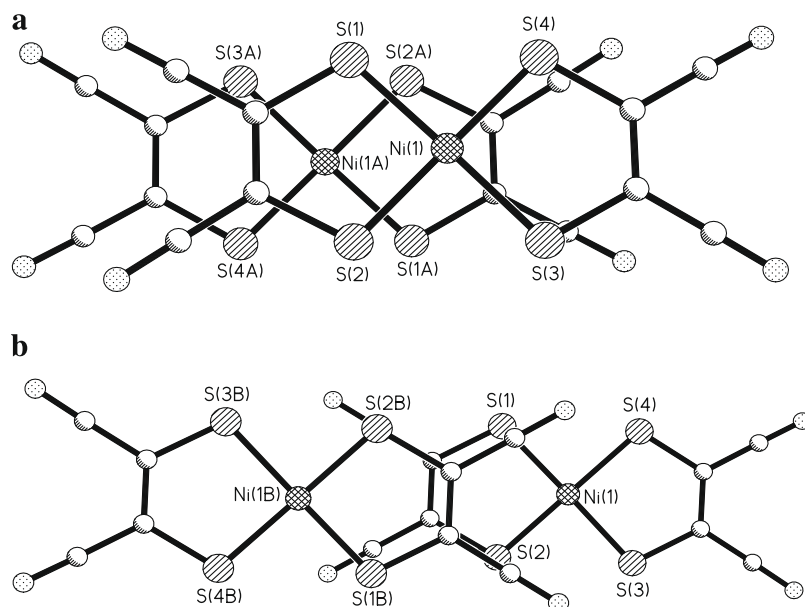


Fig. 4. (a) The Ni-ring overlapping fashion of  $[\text{Ni}(\text{mnt})_2]^-$  anions of **2**. (b) The ring–ring overlapping fashion of  $[\text{Ni}(\text{mnt})_2]^-$  anions of **2**.

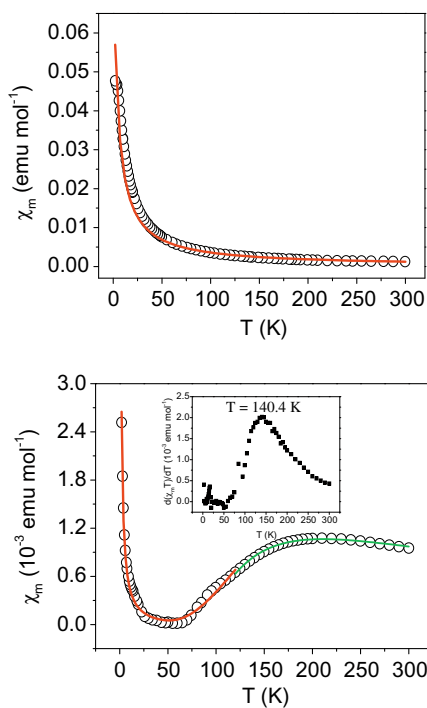


Fig. 5. Plots of  $\chi_m$  vs.  $T$  for **1(a)** and **2(b)** (inset: plot of  $d(\chi_m T)/dT$  vs.  $T$ ). The solid lines are reproduced from the theoretic calculations and detailed fitting procedure described in the text.

decreases abruptly to a minimum around 60 K, and finally increases again upon further cooling to 2 K. The room temperature  $\chi_m T$ , value of  $0.286 \text{ emu K mol}^{-1}$  is significantly lower than the expected value ( $0.375 \text{ emu K mol}^{-1}$ ) or  $\text{Ni}^{\text{III}}$  ( $s = 1/2$ ) that is magnetically isolated, and the value of  $\chi_m$  decreases to  $0.226 \text{ emu K mol}^{-1}$  around 210 K when the temperature decreases. Below this temperature, the  $\chi_m$  decreases exponentially and exhibits the characteristics of a spin-gap system [17–22]. The transition temperature is evaluated as the temperature at the maximum of the  $d(\chi_m T)/dT$  derivative, that is,  $\sim 140 \text{ K}$  (inset of Fig. 5b). From the point of view

of structure analysis for **2**, the magnetic interaction between the Ni(1) and Ni(1A) ions (Fig. 4a) is larger than that between the Ni(1) and Ni(1B) ions (Fig. 4b). Therefore, the magnetic susceptibility data in the high-temperature phase (120–300 K) of **2** can be fitted using simple dinuclear model approximation (the Hamiltonian being  $H = -2J S_A S_B$ ) (Eq. (1) [23]):

$$\chi_m = \frac{2N\beta^2 g^2}{kT} (1 - \rho) / (3 + \exp(-2J/kT)) + (N\beta^2 g^2 / 2kT) \rho \quad (1)$$

where  $N$ ,  $g$ ,  $k$ ,  $\beta$  and  $\rho$  have their usual meanings, and  $J$  is the exchange coupling parameter describing the magnetic interaction between any two neighbouring  $s = 1/2$  spins. The best-fit parameters obtained by least-squares fit are:  $g = 1.99$ ,  $J = -251.7 \text{ cm}^{-1}$ ,  $\rho = 4.8 \times 10^{-2}$  and  $R = 8.6 \times 10^{-6}$  ( $R$  is defined as  $\sum(\chi_m^{\text{calcd}} - \chi_m^{\text{obsd}})^2 / \sum(\chi_m^{\text{obsd}})^2$ ). The magnetic susceptibilities in the low-temperature phase (2–120 K) may be estimated by the formula (Eq. (2) [24]):

$$\chi_m = \alpha \exp(-\Delta/kbT) / T + C/T + \chi_0 \quad (2)$$

where  $\alpha$  is a constant value corresponding to the dispersion of excitation energy,  $\Delta$  is the magnitude of the spin-gap,  $\chi_0$  contributes from the core diamagnetism and the possible Van Vleck paramagnetism, and the other symbols have their usual meanings. The best-fitting curve is shown in Fig. 5b, and the corresponding parameters are given as follows:  $\alpha = 1.90$ ,  $\Delta/k_b = 381.4 \text{ K}$ ,  $C = 5.4 \times 10^{-3} \text{ emu K mol}^{-1}$ ,  $\chi_0 = 5.0 \times 10^{-5} \text{ emu mol}^{-1}$ , and  $R = 2.9 \times 10^{-6}$ . According to the results, the value of the parameter  $2\Delta/k_b T_c$  ( $T_c$  is the transition temperature) are estimated to be 5.43 for **2**, which is higher than the ideal value of 3.53 derived from the BCS formula in a weak coupling regime. This result thus means that the spin-gap transition is not a pure spin-Peierls transition [25,26].

Derivatives of benzylpyridinium (abbreviated as  $[\text{RBzPy}]^+$ ) have been proved to serve as flexible cations which can be adjusted *via* modifying the nature of the groups on the aromatic rings, and the molecular configuration may be determined by three dihedral angles ( $\theta_1$ ,  $\theta_2$ , and  $\theta_3$ ) [27]. When we have fixed the 2-aminopyridine ring and changed the phenyl ring into the naphthyl ring, these dihedral angles were changed from  $90.0^\circ$ ,  $0^\circ$  and  $90.0^\circ$  for **1** to  $118.0^\circ$ ,  $82.1^\circ$  and  $66.3^\circ$  for **2**. The overlapping fashions of the  $[\text{Ni}(\text{mnt})_2]^-$  anions are markedly different for **1** and **2** (Figs. 2a,

4a and b). For **2**, On the temperature is lowered, the non-uniform compression of the magnetic chain and slippage of the  $[\text{Ni}(\text{mnt})_2]^-$  stack due to the anisotropic contraction of the crystal result in the magnetic exchange constant changing and trigger a spin-gap transition.

#### 4. Conclusion

Two new molecular solids,  $[\text{BzPyNH}_2][\text{Ni}(\text{mnt})_2]$ (**1**) and  $[2\text{-NpCH}_2\text{PyNH}_2][\text{Ni}(\text{mnt})_2]$ (**2**) ( $\text{mnt}^{2-}$  = maleonitriledithiolate,  $[\text{BzPyNH}_2]^+$  = 1-benzyl-2-aminopyridinium and  $[2\text{-NpCH}_2\text{PyNH}_2]^+$  = 1-(2'-naphthylmethylene)-2-aminopyridinium) have been characterized structurally and magnetically. The Ni(III) ions of **1** and **2** form a 1D magnetic chain within a  $[\text{Ni}(\text{mnt})_2]^-$  anions column through  $\text{Ni}\cdots\text{N}$  or  $\pi\cdots\pi$  interactions. The overlapping fashions of the  $[\text{Ni}(\text{mnt})_2]^-$  anions are different when we have fixed the 2-aminopyridine ring and changed the phenyl ring into the naphthyl ring. Magnetic susceptibility measurements in the temperature range 2–300 K show that **1** displays weak antiferromagnetic coupling ( $\theta = -4.2$  K, while **2** exhibits a novel and interesting spin-gap transition around 140 K with  $\Delta/k_B = 384.1$  K.

#### Supplementary material

CCDC 711739 and 711740 contain the supplementary crystallographic data for this paper. These data can be obtained free of charge from The Cambridge Crystallographic Data Centre via [www.ccdc.cam.ac.uk/data\\_request/cif](http://www.ccdc.cam.ac.uk/data_request/cif).

#### Acknowledgements

The authors thank the Science and Technology Project (No. 2007B011000008, No. 2008B080703005) from Guangdong Science and Technology Department and the President's Science Foundation of South China Agricultural University (No. 2008X015) for financial support of this work.

#### References

- [1] N. Robertson, L. Cronin, *Coord. Chem. Rev.* 227 (2002) 93.
- [2] E. Canadell, *Coord. Chem. Rev.* 185–186 (1999) 629.
- [3] C. Rovira, *Chem. Eur. J.* 6 (2000) 1723.
- [4] T. Akutagawa, T. Nakamura, *Coord. Chem. Rev.* 226 (2002) 3.
- [5] M.M. Torrent, H. Alves, E.B. Lopes, M. Almeida, K. Wurst, J.V. Gancedo, J. Veciana, C. Rovira, *J. Solid State Chem.* 168 (2002) 563.
- [6] A.T. Coomber, D. Beljonne, R.H. Friend, J.L. Brédas, A. Charlton, N. Robertson, A.E. Underhill, M. Kurmoo, P. Day, *Nature* 380 (1996) 144.
- [7] Z.P. Ni, X.M. Ren, J. Ma, J.L. Xie, C.L. Ni, Z.D. Chen, Q.J. Meng, *J. Am. Chem. Soc.* 127 (2005) 14330.
- [8] J.L. Xie, X.M. Ren, Y. Song, Y. Zou, Q.J. Meng, *J. Chem. Soc., Dalton Trans.* (2002) 2868.
- [9] X.M. Ren, Q.J. Meng, Y. Song, C.L. Lu, C.J. Hu, X.Y. Chen, Z.L. Xue, *Inorg. Chem.* 41 (2002) 5931.
- [10] C.L. Ni, Z.P. Ni, Z.F. Tian, Q.J. Meng, *Synth. Met.* 158 (2008) 1015.
- [11] C.L. Ni, D.B. Dang, Y.Z. Li, S. Gao, Z.P. Ni, Z.F. Tian, Q.J. Meng, *J. Solid State Chem.* 178 (2005) 100.
- [12] J.L. Xie, X.M. Ren, Y. Song, W.W. Zhang, W.L. Liu, C. He, Q.J. Meng, *Chem. Commun.* (2002) 2346.
- [13] A. Davison, R.H. Holm, *Inorg. Synth.* 10 (1967) 8.
- [14] S.B. Bulgarevich, D.V. Bren, D.Y. Movshovic, P. Finocchiaro, S. Failla, *J. Mol. Struct.* 317 (1994) 147.
- [15] C.L. Ni, Y. Song, Q.J. Meng, *Chem. Phys. Lett.* 419 (2006) 351.
- [16] SHELXTL, Version 5.10. Structure Determination Software Programs, Bruker Analytical X-ray Systems, Inc., Madison, Wisconsin, USA, 2000.
- [17] Y. Fujii, T. Goto, W. Fujita, K. Awaga, *Physica B* 329–333 (2003) 973.
- [18] S. Nishihara, T. Akutagawa, T. Hasegawa, T. Nakamura, *Chem. Commun.* (2002) 408.
- [19] C. Yasuda, S. Todo, M. Matsumoto, H. Takayama, *J. Phys. Chem. Solids* 63 (2002) 1607.
- [20] S. Nishihara, T. Akutagawa, T. Hasegawa, S. Fujiyama, T. Nakamura, *J. Solid State Chem.* 168 (2002) 661.
- [21] C.L. Ni, Y.Z. Li, D.B. Dang, Z.P. Ni, Z.F. Tian, Z.R. Yuan, Q.J. Meng, *Inorg. Chem. Commun.* 8 (2005) 105.
- [22] D.B. Dang, C.L. Ni, Y. Bai, Z.F. Tian, Z.P. Ni, L.L. Wen, Q.J. Meng, S. Gao, *Chem. Lett.* 5 (2005) 680.
- [23] X.M. Ren, T. Akutagawa, S. Nishihara, T. Nakamura, *Synth. Met.* 150 (2005) 57.
- [24] L.C. Isett, D.M. Rosso, G.L. Bottger, *Phys. Rev. B* 22 (1980) 4739.
- [25] C.L. Ni, D.B. Dang, Y. Song, S. Gao, Y.Z. Li, Z.P. Ni, Z.F. Tian, L.L. Wen, Q.J. Meng, *Chem. Phys. Lett.* 396 (2004) 353.
- [26] X.M. Ren, Q.J. Meng, Y. Song, C.S. Lu, C.J. Hu, *Inorg. Chem.* 41 (2002) 5686.
- [27] X.M. Ren, S. Nishihara, T. Akutagawa, S. Noro, T. Nakamura, W. Fujita, K. Awaga, Z.P. Ni, J.L. Xie, Q.J. Meng, R.K. Kremer, *J. Chem. Soc., Dalton Trans.* (2006) 1988.